PUBLICATIONS OF THE ASTRONOMICAL SOCIETY OF THE PACIFIC, **118**: 697–705, 2006 May

Variable Unidentified Emission near 6307 Å in η Carinae[1,2]

J. C. MARTIN,[3] K. DAVIDSON,[3] F. HAMANN,[4] O. STAHL,[5] AND K. WEIS[6,7]
Received 2006 January 17; accepted 2006 March 6; published 2006 May 26

ABSTRACT. We have discovered a conspicuous unidentified variable feature near 6307 Å in the spectrum of η Carinae that is spatially unresolved from the central star and its wind ($r \lesssim 200$–300 AU). It is significant for two reasons: first, such prominent unidentified lines are now rare in this object, and second, this feature varies strongly and systematically. It exhibits a combination of characteristics that, so far as we know, are unique in η Carinae's spectrum. It may provide insights into the recurrent spectroscopic events and the star's long-term brightening.

1. INTRODUCTION

The spectrum of η Carinae has been extensively studied and characterized, but unexpected changes can happen during a spectroscopic event like the one that occurred in mid-2003. For instance, surprisingly strong high-excitation He II λ4687 briefly appeared at that time, as reported by Steiner & Damineli (2004), Stahl et al. (2005), and Martin et al. (2006); see the last of those papers for an analysis of its significance. Motivated by this example, we have examined *Hubble Space Telescope* (*HST*) data for other transient features. Our search yielded an undiagnosed emission feature at 6307 Å, with a good signal-to-noise ratio (S/N) and unusual behavior.

These data were obtained with the Space Telescope Imaging Spectrograph (STIS), whose high spatial resolution allowed us to examine the central star itself (or rather its inner wind) apart from the bright nearby ejecta, which contaminate all ground-based spectroscopy of η Car (Fig. 1).

In the STIS CCD data, the 6307 Å feature is spatially unresolved from the continuum emission of the central star and its wind. It does not match any of the known atomic or molecular transitions of any species that we expect to find in the spectrum (see Thackeray [1953], Zethson [2001a], and Wallerstein et al. [2001] for extensive lists of species identified in η Car; the relevant part of Zethson's line list is reproduced in Table 1). This is a significant discovery because, unlike the few other noticeable lines that have not yet been identified, the 6307 Å emission varies conspicuously. It is obviously correlated with η Car's 5.5 yr spectroscopic period; indeed, it temporarily disappeared during the 1998 and 2003 spectroscopic events. Moreover, following the 2003 event, this feature became much stronger than it had been in the previous cycle, possibly indicating a link with the rapid brightening and other mysterious developments that have been superimposed on the 5.5 yr cycle since the mid-1990s (Davidson et al. 1999, 2005; Martin & Koppelman 2004). Altogether, it is unique in the small set of lines that remain unidentified in η Car's spectrum.

2. THE DATA

2.1. Spectra

The *HST* STIS spectra in this paper were obtained as part of the η Carinae *HST* Treasury Project (Davidson 2004) and were reduced using a modified version of the Goddard CALSTIS reduction pipeline (Table 2). The modified pipeline uses the normal *HST* bias subtraction, flat-fielding, and cosmic-ray rejection procedures, with the addition of improved pixel interpolation and improved bad/hot pixel removal. Information regarding these modifications can be found online at our Web site[8] and in a forthcoming publication (K. Davidson et al. 2006, in preparation). The spectra were reduced and extracted using approximately the same parameters used by Martin et al. (2006). Each one-dimensional STIS spectrum discussed here is essentially a $0\farcs1 \times 0\farcs25$ spatial sample: the pixel size is about $0\farcs05$, the slit width is about two CCD columns, each spectral extraction sampled five CCD rows, and the spectral resolution is roughly 52 km s^{-1} at 6307 Å. We applied an aperture (extraction height) correction to the absolute flux, based on an observation of the spectrophotometric standard

[1] This research is part of the *Hubble Space Telescope* Treasury Project for η Carinae, supported by grants GO-9420 and GO-9973 from the Space Telescope Science Institute (STScI), which is operated by the Association of Universities for Research in Astronomy, Inc., under NASA contract NAS 5-26555.

[2] Partially based on observations obtained with UVES at the ESO Very Large Telescope, Paranal, Chile (proposals 70.D-0607[A], 71.D-0168[A], and 72.D-0524[A]).

[3] School of Physics and Astronomy, University of Minnesota, 116 Church Street, SE, Minneapolis, MN 55455; martin@etacar.umn.edu.

[4] Department of Astronomy, University of Florida, P.O. Box 112055, Gainesville, FL 32611.

[5] Landessternwarte Heidelberg, Königsstuhl, D-69117 Heidelberg, Germany.

[6] Astronomisches Institut, Ruhr-Universität Bochum, Universitätsstrasse 150, D-44780 Bochum, Germany.

[7] Lise Meitner Fellow.

[8] See http://etacar.umn.edu.

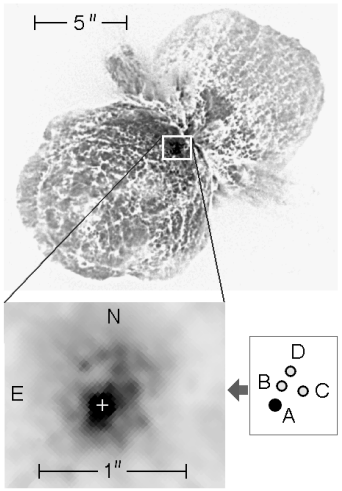

FIG. 1.—Spatial distribution of ejecta mentioned in text. *Top*: Map of the Homunculus based on *HST* WFPC2 images. The small white rectangle is the enlarged region shown below. *Bottom left*: *HST* ACS image of the inner region, using the F330W filter (near-UV) in 2005. *Bottom right*: Relative locations of the slow-moving "Weigelt blobs" B, C, and D specified by Hofmann & Weigelt (1988), expanded 20% to allow for motions. The spatial scale throughout this figure is adjusted to epoch 2005.

BD +75 325 with the same slit and extraction parameters. Such details have little effect on the main results of this paper.

In addition to the *HST* STIS spectra, we used spectra of the central star observed with the ESO VLT Ultraviolet-Visual Echelle Spectrograph (UVES). That observing program is described in detail by Weis et al. (2005a, 2005b). Each one-dimensional UVES spectrum is a 0.″30 × 0.″91 spatial sample: the pixel size is about 0.″182, the slit width is just under two CCD columns, each spectral extraction sampled five CCD rows, the seeing ranged from 0.″5 to 1.″3, and the spectral resolution is roughly 3.75 km s^{-1} at 6307 Å. We corrected the wavelength scale to the heliocentric reference frame using the IRAF procedure `rvcorrect`. These spectra are not absolute-flux calibrated.

In ground-based spectra, such as those from the VLT UVES, strong atmospheric absorption bands and emission lines from the bright ejecta make it difficult at some wavelengths to detect even dramatic changes in the spectrum of the central star. In the VLT UVES spectra, sharp-lined atmospheric O_2 absorption is observed around 6307 Å, and sharp nebular Fe II λ6307.04 and Cr II λ6307.39 that are formed in the nearby ejecta are blended with the stellar spectra. The *HST* STIS spectra are unlike ground-based observations, in that they are free of atmospheric absorption and specifically include only the region within $r \approx 200$–300 AU of the central star. Here "the star" or "η Carinae" means the central object and its wind, excluding the bright ejecta and Homunculus Nebula (Fig. 1). If the star is a double, then it is unresolved by the *HST*.

TABLE 1
NARROW NEBULAR EMISSION LINES IDENTIFIED BY ZETHSON NEAR 6307 Å

λ_{obs} (Å)	Species	Transition	λ_{lab} (Å)	Note[a]
6256.56	Fe II(34)	$b\ ^4F_{3/2}$–$z\ ^6D_{3/2}$	6257.08	
6261.88	[Fe II](44F)	$a\ ^2G_{9/2}$–$b\ ^2F_{5/2}$	6265.93	
6265.17	[V II]	$a\ ^3D_1$–$b\ ^1F_3$	6265.93	id?
	[V II]	$b\ ^3G_3$–$d\ ^3P_1$	6266.33	id?
	[V II]	$a\ ^3G_5$–$d\ ^3F_4$	6266.34	id?
6270.62	Fe II	$b\ ^2H_{11/2}$–$z\ ^6P_{3/2}$	6271.70	
6276.44	[Fe II](15F)	$a\ ^4F_{7/2}$–$a\ ^2P_{3/2}$	6277.2	
6280.81	[Fe II]	$a\ ^2D2_{3/2}$–$a\ ^2S_{1/2}$	6281.69	
	Fe II]	$b\ ^4F_{5/2}$–$z\ ^6D_{5/2}$	6281.56	
6287.00	[Mn II]	$a\ ^5D_2$–$a\ ^3P_1$	6287.77	
6292.65	Fe II	$(^5D)4d\ ^4P_{3/2}$–$(^5D_0)4f^2[3]_{5/2}$	6293.57	$?E_u$
6297.32	Unidentified	…	…	
6301.14	[O I](1F)	$2p^4\ ^3P_2$–$2p^4\ ^1D_2$	6302.05	
6306.3	Fe II(200)	$c\ ^4F_{9/2}$–$x\ ^4F_{9/2}$	6307.47	
	Cr II	$b\ ^2P_{3/2}$–$y\ ^2P_{3/2}$	6307.39	
6308.51	Fe II(34)	$b\ ^4F_{7/2}$–$z\ ^6D_{7/2}$	6309.27	
6312.82	[S III](3F)	$3p^2\ ^1D_2$–$3p^2\ ^1S_0$	6313.81	Not in 98
6318.77	Fe II	$z\ ^4D_{7/2}$–$c\ ^4D_{7/2}$	6319.73	$4p$–$4s$
6347.95	Si II(2)	$4s\ ^2S_{1/2}$–$4p\ ^2P_{3/2}$	6348.84	
6357.83	Fe II	$(^5D)4d\ ^4P_{5/2}$–$(^5D_2)4f^2[4]_{7/2}$	6358.92	$?E_u$
	[Mn II]	$a\ ^5D_0$–$a\ ^3P_1$	6359.21	

NOTE.—Emission-line data from Zethson (2001a).

[a] Taken from the Notes column of Zethson's tables: id? = uncertain identification; $?E_u$ = Fe II and Cr II transitions with an upper level ≥10 eV, and the excitation mechanism is "questionable"; Not in 98 = not present in the spectrum observed just after the 1998.0 spectroscopic event; $4p$–$4s$ = a $4p$–$4s$ transition.

2.2. Photometry

Figure 5 uses data from the *HST* Advanced Camera for Surveys (ACS) High Resolution Channel (HRC) that were obtained as part of the *HST* Treasury Project. These data are summarized in Table 3 of Martin & Koppelman (2004). The bias-corrected, dark-subtracted, and flat-fielded images were obtained from the Space Telescope Science Institute via the Multimission Archive (MAST; Sirianni et al. 2005)[9] and measured with a 0.″3 radius (~10 ACS HRC pixels) weighted aperture described by Martin & Koppelman (2004). The measured flux is corrected to an infinite aperture using factors we derived following Sirianni et al. (2005) from archived observations of the star GD 71. The corrected fluxes were converted to the STMAG system (Sirianni et al. 2005) using the standard photometry key words provided by the STScI reduction pipeline in the FITS headers.

The ACS HRC data are supplemented by photometry synthesized from flux-calibrated STIS CCD spectra. A summary of the spectra is given in Table 2. They were extracted with a cross-dispersion weighting function that matched the 0.″3 aperture used to measure the ACS HRC images. We applied an

[9] See http://archive.stsci.edu.

TABLE 2
HST STIS DATA

Root Name	MJD	Slit	Slit Angle[a] (deg)	Grating	Central λ (Å)	Exposure Length (s)
6307 Å Observations						
o4j801120	50,891.7	52 × 0.1	−28	G750M	6252	9.4
o556020p0	51,230.6	52 × 0.1	−28	G750M	6252	8.0
o5kz010m0	51,623.9	52 × 0.1	−28	G750M	6252	10.0
o62r010l0	52,016.8	52 × 0.1	+22	G750M	6252	10.0
o6ex020l0	52,294.1	52 × 0.1	−82	G750M	6252	8.0
o6mo02150	52,459.7	52 × 0.1	+69	G750M	6252	8.0
o8gm12050	52,682.9	52 × 0.1	−57	G750M	6252	8.0
o8gm330r0	52,776.6	52 × 0.1	+38	G750M	6252	8.0
o8gm521s0	52,792.0	52 × 0.1	+62	G750M	6252	8.0
o8gm520h0	52,812.2	52 × 0.1	+70	G750M	6252	15.0
o8ma820a0	52,852.0	52 × 0.1	+105	G750M	6252	8.0
o8ma920z0	52,904.5	52 × 0.1	+153	G750M	6252	8.0
o8ma940r0	53,071.3	52 × 0.1	−28	G750M	6252	10.0
Fe II λ5529 Observations						
o4j8010d0	50,891.5	52 × 0.1	−28	G750M	5734	15.0
o55602090	51,230.5	52 × 0.1	−28	G750M	5734	15.0
o62r01090	52,016.8	52 × 0.1	+21	G750M	5734	8.0
o6ex030b0	52,183.1	52 × 0.1	+165	G750M	5734	15.0
o6ex02090	52,294.0	52 × 0.1	−82	G750M	5734	6.0
o6mo020i0	52,459.6	52 × 0.1	+69	G750M	5734	9.0
o8gm120a0	52,682.9	52 × 0.1	−57	G750M	5734	6.0
o8gm210d0	52,727.3	52 × 0.1	−28	G750M	5734	9.0
o8gm410d0	52,764.4	52 × 0.1	+27	G750M	5734	9.0
o8gm320i0	52,778.6	52 × 0.1	+38	G750M	5734	9.0
o8gm520i0	52,791.8	52 × 0.1	+62	G750M	5734	9.0
o8gm620i0	52,814.0	52 × 0.1	+70	G750M	5734	9.0
o8ma720h0	52,825.4	52 × 0.1	+69	G750M	5734	9.0
o8ma820j0	52,852.0	52 × 0.1	+105	G750M	5734	6.0
o8ma920b0	52,904.4	52 × 0.1	+153	G750M	5734	6.0
o8ma830d0	52,960.7	52 × 0.1	−142	G750M	5734	8.0
o8ma94080	53,071.3	52 × 0.1	−28	G750M	5734	6.0
Spectra Used to Synthesize ACS HRC F250W Fluxes						
o8gm12030	52,682.9	52 × 0.1	−57	G230MB	2836	300.0
o8gm12090	52,682.9	52 × 0.1	−57	G230MB	2557	800.0
o8gm120b0	52,682.9	52 × 0.1	−57	G430M	3680	52.0
o8gm120c0	52,682.9	52 × 0.1	−57	G230MB	2697	340.0
o8gm120d0	52,682.9	52 × 0.1	−57	G430M	3423	90.0
o8gm120h0	52,683.0	52 × 0.1	−57	G230MB	1995	600.0
o8gm120l0	52,683.0	52 × 0.1	−57	G230MB	2135	600.0
o8gm120n0	52,683.0	52 × 0.1	−57	G430M	3165	90.0
o8gm120r0	52,683.0	52 × 0.1	−57	G230MB	2416	320.0
o8gm120t0	52,683.0	52 × 0.1	−57	G230MB	2976	340.0
o8gm120w0	52,683.0	52 × 0.1	−57	G230MB	2276	600.0
o8gm33020	52,776.4	52 × 0.1	+38	G230MB	2135	300.0
o8gm33060	52,776.4	52 × 0.1	+38	G430M	3165	90.0
o8gm33090	52,776.5	52 × 0.1	+38	G230MB	3115	300.0
o8gm330e0	52,776.5	52 × 0.1	+38	G230MB	2416	320.0
o8gm330i0	52,776.5	52 × 0.1	+38	G230MB	2976	320.0
o8gm330n0	52,776.5	52 × 0.1	+38	G230MB	2276	300.0
o8gm32050	52,776.6	52 × 0.1	+38	G230MB	2836	300.0
o8gm320h0	52,778.6	52 × 0.1	+38	G230MB	2557	400.0
o8gm320l0	52,778.7	52 × 0.1	+38	G430M	3680	52.0
o8gm320m0	52,778.7	52 × 0.1	+38	G230MB	2697	340.0
o8gm320p0	52,778.7	52 × 0.1	+38	G430M	3423	90.0
o8gm320x0	52,778.7	52 × 0.1	+38	G230MB	1995	300.0
o8gm52050	52,791.7	52 × 0.1	+62	G230MB	2836	300.0
o8gm520h0	52,791.8	52 × 0.1	+62	G230MB	2557	400.0

TABLE 2 (*Continued*)

Root Name	MJD	Slit	Slit Angle[a] (deg)	Grating	Central λ (Å)	Exposure Length (s)
o8gm520l0	52,791.8	52 × 0.1	+62	G430M	3680	52.0
o8gm520m0	52,,791.8	52 × 0.1	+62	G230MB	2697	340.0
o8gm520p0	52,791.8	52 × 0.1	+62	G430M	3680	90.0
o8gm520x0	52,791.8	52 × 0.1	+62	G230MB	1995	300.0
o8gm52100	52,791.9	52 × 0.1	+62	G230MB	2135	400.0
o8gm52170	52,791.9	52 × 0.1	+62	G430M	3165	90.0
o8gm52180	52,791.9	52 × 0.1	+62	G230MB	3115	300.0
o8gm521f0	52,791.9	52 × 0.1	+62	G230MB	2416	320.0
o8gm521j0	52,791.9	52 × 0.1	+62	G230MB	2976	340.0
o8gm521o0	52,792.0	52 × 0.1	+62	G230MB	2276	300.0
o8gm63040	52,812.1	52 × 0.1	+70	G230MB	2416	350.0
o8gm63080	52,812.2	52 × 0.1	+70	G230MB	2976	320.0
o8gm630d0	52,812.2	52 × 0.1	+70	G230MB	2836	300.0
o8gm62050	52,813.7	52 × 0.1	+70	G230MB	2836	300.0
o8gm620h0	52,814.0	52 × 0.1	+70	G230MB	2557	400.0
o8gm620l0	52,814.1	52 × 0.1	+70	G430M	3680	52.0
o8gm620m0	52,814.1	52 × 0.1	+70	G230MB	2697	340.0
o8gm620p0	52,814.1	52 × 0.1	+70	G430M	3423	90.0
o8gm620x0	52,814.2	52 × 0.1	+70	G230MB	1995	300.0
o8gm62100	52,814.2	52 × 0.1	+70	G230MB	2135	300.0
o8gm62140	52,814.2	52 × 0.1	+70	G430M	3165	90.0
o8ma82060	52,851.9	52 × 0.1	+105	G230MB	2836	300.0
o8ma820i0	52,852.0	52 × 0.1	+105	G230MB	2557	400.0
o8ma820m0	52,852.1	52 × 0.1	+105	G430M	3680	52.0
o8ma820n0	52,852.1	52 × 0.1	+105	G230MB	2697	340.0
o8ma820q0	52,852.1	52 × 0.1	+105	G430M	2697	90.0
o8ma820y0	52,852.2	52 × 0.1	+105	G230MB	1995	300.0
o8ma82110	52,852.2	52 × 0.1	+105	G230MB	2135	300.0
o8ma821a0	52,852.3	52 × 0.1	+105	G430M	3165	90.0
o8ma821b0	52,852.3	52 × 0.1	+105	G230MB	2416	320.0
o8ma821i0	52,852.4	52 × 0.1	+105	G230MB	2976	300.0
o8ma821m0	52,852.4	52 × 0.1	+105	G230MB	2276	300.0
o8ma92040	52,940.3	52 × 0.1	+153	G230MB	2836	300.0
o8ma920a0	52,940.3	52 × 0.1	+153	G230MB	2557	800.0
o8ma920c0	52,940.4	52 × 0.1	+153	G430M	3680	52.0
o8ma920d0	52,940.4	52 × 0.1	+153	G230MB	2697	340.0
o8ma920e0	52,940.4	52 × 0.1	+153	G430M	3423	90.0
o8ma920i0	52,940.4	52 × 0.1	+153	G230MB	1995	600.0
o8ma920m0	52,940.4	52 × 0.1	+153	G230MB	2135	600.0
o8ma920o0	52,940.4	52 × 0.1	+153	G430M	3350	90.0
o8ma920p0	52,940.4	52 × 0.1	+153	G230MB	3115	300.0
o8ma920s0	52,940.5	52 × 0.1	+153	G230MB	2416	600.0
o8ma920u0	52,940.5	52 × 0.1	+153	G230MB	2976	340.0
o8ma920x0	52,940.5	52 × 0.1	+153	G230MB	2276	300.0
o8ma94020	53,071.3	52 × 0.1	−28	G230MB	2836	320.0
o8ma94070	53,071.3	52 × 0.1	−28	G230MB	2557	410.0
o8ma94090	53,071.3	52 × 0.1	−28	G430M	2557	52.0
o8ma940a0	53,071.3	52 × 0.1	−28	G430M	3423	90.0
o8ma940e0	53,071.3	52 × 0.1	−28	G230MB	2697	323.0
o8ma940h0	53071.3	52 × 0.1	−28	G430M	3165	90.0
o8ma940i0	53,071.3	52 × 0.1	−28	G230MB	2135	320.0
o8ma940m0	53,071.3	52 × 0.1	−28	G230MB	2416	450.0

[a] The slit angle is measured from north through east. All slits are peaked up on the central star.

aperture (extraction height) correction based on an observation of the spectrophotometric standard star BD +75 325, with the same slit and extraction techniques. The spectra were convolved with the published ACS HRC filter and CCD response functions and then integrated to obtain synthetic fluxes. Finally, the synthetic fluxes were adjusted to the STMAG system by comparing the synthetic results to results from ACS HRC observations made on the same day (MJD 52,682).

3. OVERVIEW OF THE FEATURE

The unidentified emission feature appeared in the wing of the Fe II λ6319 line near 6307 Å (Figs. 2 and 3 and Table 3). It had a FWHM of about 150–180 km s^{-1}, which is narrower than the stellar wind features (FWHM ≈ 300–500 km s^{-1}) but is significantly broader than the nebular emission from the surrounding bright ejecta (FWHM ≈ 10 km s^{-1}; Zethson 2001a).[10]

The feature is also present in the spectrum of the star reflected by the Homunculus lobes (see the VLT UVES FOS4 slit setting described by Weis et al. [2005a]). The equivalent width of the feature is smaller there. However, there is no variation of its profile along the UVES slit, except for the radial velocity shift introduced by the motion of the reflecting ejecta. This leads us to conclude that unlike Hα (Smith et al. 2003), there is no obvious variation of this feature with stellar latitude.

4. IDENTIFICATION

We have been unable to find any known transitions consistent with other lines present in the spectrum that match this feature. We ruled out S II λ6307, because none of the associated transitions with similar levels and oscillator strengths at 6314.4, 6288.6, or 6288.0 Å appeared in the spectrum. Another possible identification may be [O I] λ6302.0, redshifted by 100–200 km s^{-1}. Nearly all the atomic oxygen in the wind of the central star is probably ionized. O I λ1302, λ1307, and λ1306 are present in data from the *HST* STIS Multianode Microchannel Array (MAMA), but they are *blueshifted* by 400–500 km s^{-1}. However, the [O I] λ6365 is not present, and a 100 km s^{-1} redshift would be anomalous. Therefore, the 6307 Å emission is probably not [O I] λ6302.0. Thackeray (1953), Damineli et al. (1998), Wallerstein et al. (2001), and Zethson (2001a) reported [O I] λ6302.0 in their spectra, but the line they describe is narrow, redshifted, and originates in the surrounding bright ejecta, not the central star (Fig. 1). Its wavelength obviously differs from the feature that we discuss.

We considered emission pumped by Lyα, since η Car is a significant source of Lyα emission, and resonance with that emission plays a role in the formation of other features (Martin et al. 2006; Johansson & Hamann 1993; Zethson et al. 2001b). We found three transitions between 6305 and 6309 Å that are resonant with absorption features within 3 Å of Lyα: Cr II λ6305.75 (resonant with λ1213.499), Cr III] λ6306.8 (resonant with λ1215.781), and Fe III] λ6306.43 (resonant with λ1213.41). The oscillator strengths have not been measured for any of these transitions. While all these species appear in the nebular spectra of the nearby ejecta, they are not found in the stellar spectrum. Furthermore, we do not see these specific transitions in the nebular spectra along with other previously identified resonance-type features. Altogether, it is difficult to judge the likelihood of these possible identifications. However, there is some appeal to identifying it as an ionized metal line,

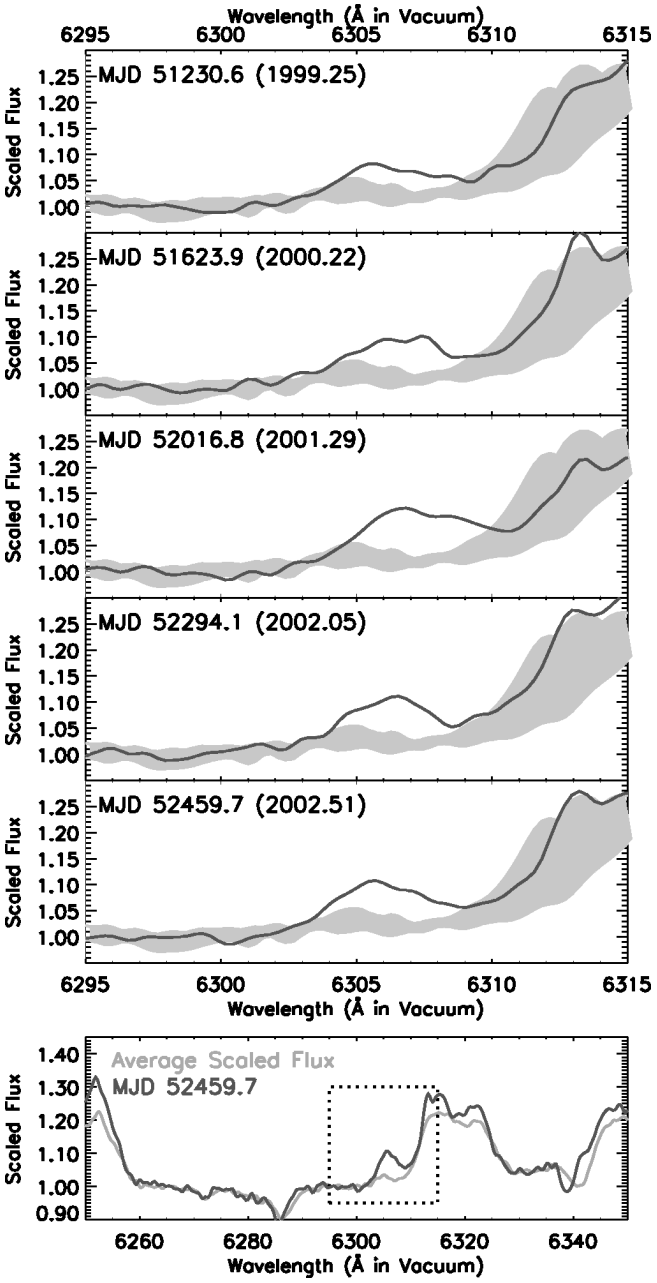

FIG. 2.—Plots of the *HST* STIS spectra. *Top panels*: Plots of the 6307 Å emission on the dates that it was unambiguously present. The gray region in each plot gives the range of relative flux values when the emission was definitely not present during the 2003.5 spectroscopic event. *Bottom panel*: Plot of the average scaled flux and the flux recorded on MJD 52,459.7 over an expanded wavelength range. The dotted box marks the area plotted in the panels above.

[10] The spectral resolution of the STIS was roughly 52 km s^{-1} at 6307 Å. Therefore, the spectral width of the nebular emission lines is not resolved in the STIS CCD data.

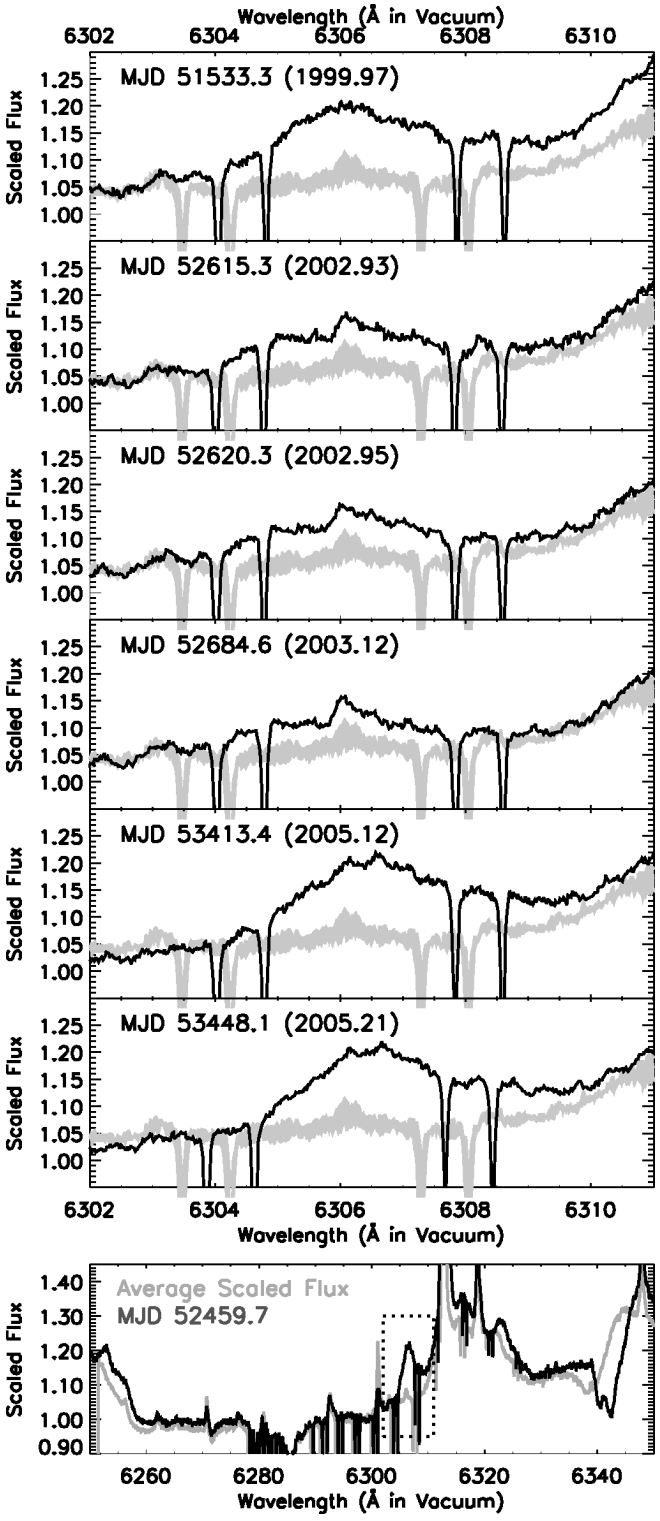

FIG. 3.—Same as Fig. 2, but for VLT UVES spectra.

since aspects of its variability are similar to those exhibited by the broad components of the Fe II lines and the metal absorption forest around 2500 Å (see § 5).

There is an emission line in the spectrum of the surrounding ejecta and Weigelt knots at 6306.3 Å, which Zethson (2001a) identified as Fe II λ6307.04 and Cr II λ6307.39 (Table 1). The line in the spectrum of the ejecta has a much sharper profile (FWHM ≈ 10 km s^{-1}) than 6307 Å in the spectrum of the star. Fe II λ6307.0 and Cr II λ6307.4 are also clearly formed in the area of extended emission within half an arcsecond of the star that is resolved by the *HST* STIS. They are not found in the spectrum of the star itself, whereas the region emitting 6307 Å is spatially unresolved from the central star (Fig. 1).

5. VARIABILITY OF THE FEATURE

The 6307 Å feature *disappeared* during the 1998.0 and 2003.5 spectroscopic events (Fig. 4) at the same time that the hydrogen Balmer absorption strengthened and broad, high-excitation emission (such as He I) weakened. It gradually declined in flux over the 6 months prior to the 2003.5 event, but just before disappearing completely, its decline was interrupted by a brief upward tick in brightness lasting a few weeks (Fig. 5). The only other component of the spectrum exhibiting similar behavior just prior to the event is the "iron curtain" of blanketed near-UV (NUV) absorption. One plausible explanation for this brief "hiccup" is a sudden change in ionization caused by an increase in the ionizing flux from the central star. In that case, 6307 Å is a metal line whose population is markedly increased as the species in the "iron curtain" are further ionized and temporarily depleted.

The 6307 Å feature also evolved much more than most other lines between the spectroscopic events. A similar degree of activity is observed in the broad components of the Fe II lines formed in the central star's wind (Fig. 6). Note that around 2001 (at a time between spectroscopic events), 6307 Å is anticorrelated with Fe II emission. Like the NUV flux, a rise in 6307 Å brightness was anticorrelated with Fe II emission.

The aspects of variability that 6307 Å shares with Fe II indicate that it is probably also an ionized metal line formed in the stellar wind. The most viable candidates are the transitions we noted as being in resonance with Lyα (Cr II λ6305.75, Cr III] λ6306.8, and Fe III] λ6306.43). For obvious reasons, Fe III] λ6306.43 is the most enticing option. Unfortunately, the atomic data for that transition are lacking, so we are unable to confirm our suspicions.

6. MIDCYCLE PHENOMENA: EVIDENCE FOR EXTRACYCLICAL PROCESSES?

In most proposed explanations of the 5.5 yr spectroscopic period *there is no obvious reason to expect much variability midcycle*; e.g., during 1999–2001, halfway between the 1998.0 and 2003.5 spectroscopic events. In the most popular scenario describing these events, the cycle is regulated by a companion

TABLE 3
MEASURED PROPERTIES OF 6307 Å

MJD	Year	Telescope	Centroid (Å)	Line Flux[a] (ergs cm^{-2} s^{-1}) × 10^{-13}	Line EW[a] (Å)
50,891.7	1998.21	*HST* STIS	...	2.98 ± 1.52	−0.01 ± 0.05[b]
51,230.6	1999.14	*HST* STIS	6306.88 ± 0.19	9.77 ± 2.66	0.19 ± 0.05
51,533.3	1999.97	VLT UVES	6306.80 ± 0.08	...	0.19 ± 0.05[b]
51,623.9	2000.22	*HST* STIS	6306.95 ± 0.19	8.89 ± 1.36	0.19 ± 0.03
52,016.8	2001.29	*HST* STIS	6307.32 ± 0.19	22.62 ± 1.63	0.39 ± 0.03
52,294.1	2002.05	*HST* STIS	6306.90 ± 0.19	14.91 ± 1.78	0.26 ± 0.03
52,459.7	2002.51	*HST* STIS	6306.75 ± 0.19	14.92 ± 3.20	0.24 ± 0.05
52,615.3	2002.93	VLT UVES	6306.50 ± 0.08	...	0.20 ± 0.06
52,620.3	2002.95	VLT UVES	6306.69 ± 0.08	...	0.24 ± 0.05
52,682.9	2003.12	*HST* STIS	6306.75 ± 0.19	7.62 ± 2.56	0.14 ± 0.05
52,684.6	2003.12	VLT UVES	6306.41 ± 0.08	...	0.14 ± 0.05
52,776.6	2003.24	*HST* STIS	...	1.79 ± 3.56	0.03 ± 0.06
52,788.6	2003.40	VLT UVES	...	...	0.05 ± 0.06
52,792.0	2003.42	*HST* STIS	...	4.65 ± 2.46	0.07 ± 0.04
52,794.5	2003.42	VLT UVES	...	...	−0.01 ± 0.04
52,812.2	2003.47	*HST* STIS	...	3.61 ± 2.98	0.05 ± 0.04
52,825.5	2003.51	VLT UVES	...	...	−0.07 ± 0.05
52,852.0	2003.58	*HST* STIS	...	−1.90 ± 2.87	−0.03 ± 0.04
52,904.5	2003.72	*HST* STIS	...	−2.19 ± 3.60	−0.03 ± 0.04
53,055.6	2004.14	VLT UVES	...	...	0.05 ± 0.04
53,071.3	2004.18	*HST* STIS	...	5.41 ± 3.22	0.06 ± 0.03
53,413.4	2005.12	VLT UVES	6306.99 ± 0.08	...	0.44 ± 0.06
53,448.1	2005.21	VLT UVES	6306.93 ± 0.08	...	0.39 ± 0.04

[a] Fluxes and equivalent widths are expressed relative to the continuum, with values greater than zero denoting excess flux above the continuum. Only the STIS CCD data are absolute flux calibrated.

[b] The wing of Fe II λ6319 was brighter than normal at this time, so that it interfered with the measurement of the equivalent width of the feature.

star in a highly eccentric orbit, as sketched in Figure 7. At distances of 20–30 AU from the primary star, where the hypothetical companion should have been during 1999–2001, relevant wind densities are factors of 30 to 100 smaller than at periastron. Column densities are correspondingly small, and the motion is quite slow. Therefore, we do not expect orbital motion alone to precipitate appreciable spectroscopic changes during that part of the cycle. Analogous comments can be made if the 5.5 yr period is a single-star thermal/rotational recovery cycle between outbursts, although such models are admittedly less definite. For these reasons, any rapid or pronounced changes observed in 1999–2001 were most likely *not* due to the 5.5 yr cycle; instead, they probably give us information about LBV-like random fluctuations in the stellar wind. If this statement is wrong, then the midcycle variations reveal an aspect of the cycle that has no explanation in any of the proposed models. In either case, it is important to study the features that did vary then. Among them, the unidentified 6307 Å feature varied the most.

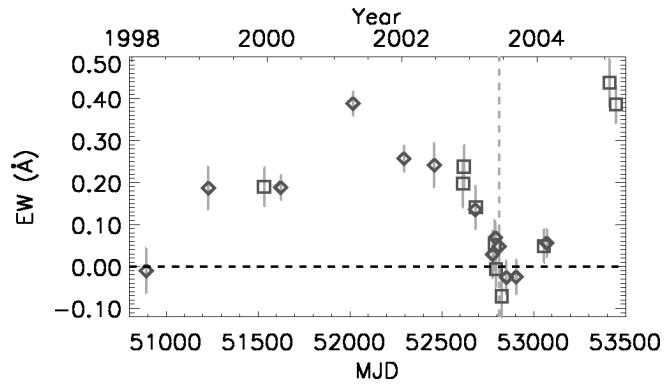

FIG. 4.—Equivalent width of 6307 Å emission in the *HST* STIS data (*diamonds*) and VLT UVES (*squares*) in the spectrum of the central star vs. time. The vertical ticks on each point are 1 σ error bars given in Table 3. The dashed vertical line marks the time of the 2003.5 spectroscopic event.

In our *HST* STIS data during the 1998–2003 cycle, this line was brightest at 2001.29 (MJD 52,016.8). Our temporal sampling was too sparse to indicate the true peak, but on that occasion the line was more than twice as strong as it had been in 1999–2000 (Fig. 4).

Meanwhile, several other changes occurred in 2001, at about the same time as the 6307 Å maximum:

1. A 0.05 mag dip in *J*, *H*, and *K* brightness (Whitelock et al. 2004);

2. A roughly 20% increase in NUV flux around 1800 Å over the course of 9 months;

3. A 15%–20% fluctuation in flux emitted in the broad com-

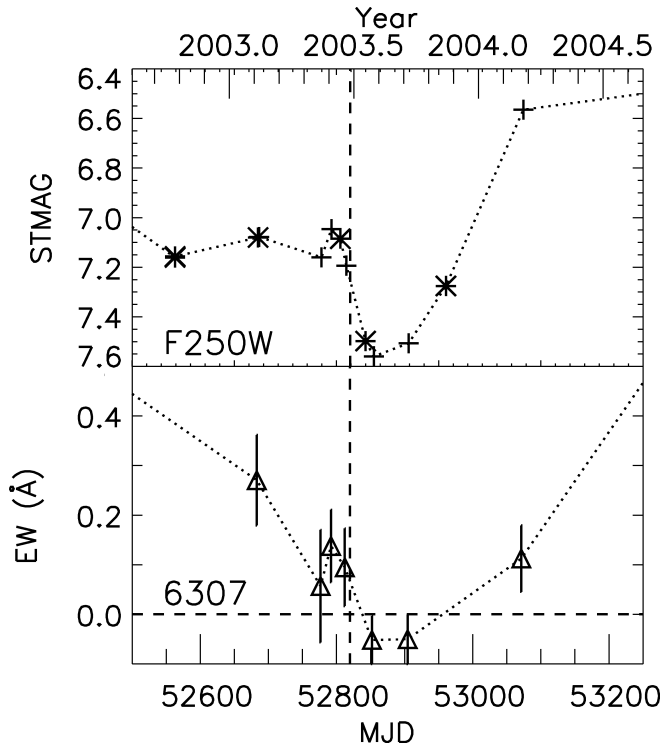

FIG. 5.—*Top*: NUV in the F250W filter, measured with the ACS HRC (*asterisks*) and synthesized from flux-calibrated STIS CCD spectra (*plus signs*). The statistical 1 σ error of each data point is 0.01–0.02 mag (smaller than the size of the symbols). *Bottom*: Equivalent width of 6307 Å measured in the STIS CCD spectra (*triangles*), with 1 σ error bars estimated from the S/N of the continuum. The vertical dashed line marks the time of the disappearance of the He I line on MJD 52,819.8 during the 2003.5 event.

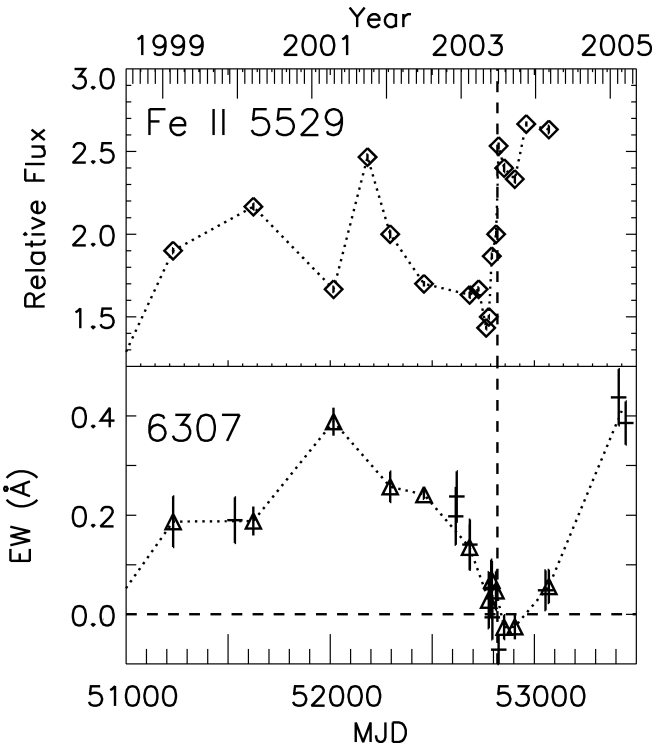

FIG. 6.—*Top*: Fe II λ5529 flux (continuum subtracted) measured in STIS CCD spectra. The 1 σ error in these data are about the size of the plotted symbols. *Bottom*: Equivalent width of 6307 Å measured in STIS CCD spectra (*triangles*) and VLT UVES spectra (*crosses*), with 1 σ error bars. The vertical dashed line marks the time of the 2003.5 event.

ponents of the Fe II lines formed in the stellar wind over the course of 9 to 12 months (see Fig. 6);

4. A 20%–30% decrease in hydrogen Balmer P Cygni absorption (Davidson et al. 2005);

5. A 10%–20% increase in the total hydrogen Balmer emission flux (Davidson et al. 2005); and

6. A sudden and significant increase in the strength of the narrow -140 km s^{-1} absorption feature in the hydrogen Balmer lines.

While these events were simultaneous, we have no proof that they are physically related. There is no clear reason or explanation why any feature should undergo significant change in the *middle* of the spectroscopic cycle. As noted, in almost any binary star model of the 5.5 yr cycle, the two components were far apart and moving slowly in 2001. The moderate changes listed above may perhaps be ascribed to ordinary LBV-like fluctuations. Although taken all together and at the same time, they are suggestive of some other process at work in addition to the spectroscopic cycle. This aspect of the overall problem of midcycle behavior has received little attention to date.

After reaching maximum, the emission feature slowly faded over the next 2 years, until it disappeared completely in the lead-up to the 2003.5 event. After the event, the feature recovered. However on MJD 53,413 and MJD 53,448, the flux of the feature was more than twice that seen at the same phase a cycle earlier (approximately MJD 51,500). The fact that the behavior of the feature appears to be different from cycle to cycle suggests that it is affected by some additional parameter; i.e., the long-term brightening trend of the central star.

7. SUMMARY

We have discovered a previously unidentified emission feature in the spectrum of η Carinae: a single emission line at 6307 Å. This feature is important for a number of reasons:

1. The visual light spectrum of η Carinae has been extensively studied, and only about 3% of the features remain unidentified (Zethson 2001a).

2. This feature's variability appears to be associated with the variability of Fe II in the wind of the central star.

3. It evolves in a unique way with time and thus may provide clues to the nature of the spectroscopic cycle and/or a long-term brightening trend.

4. The peak in the flux of the feature coincided with several

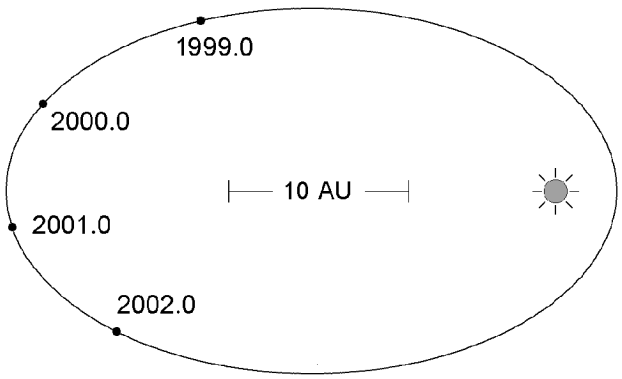

FIG. 7.—Orbital plot for the hypothetical secondary companion. The secondary was well separated from the primary when the 6306 Å feature was still varying between 1999.0 and 2002.0. The time of periastron is uncertain by several weeks but has little effect on this sketch.

other mid–spectroscopic cycle changes in the spectrum that we cannot explain.

5. The 6307 Å feature is associated with the spectroscopic cycle, but its behavior does not reproduce exactly from one cycle to the next.

This feature is visible in some spectra of the central star and its wind, but not in others, during the last 7 years. We are unable to match it to any published atomic or molecular transitions of species that we expect to find in the spectrum, based on other lines present. Its unidentified and transient nature makes it fairly unique in the spectrum of η Carinae. Its disappearance and reappearance correlates with the spectroscopic events, implying that it is associated with the spectroscopic cycle. Its midcycle peak and cycle-to-cycle changes are also sufficiently different from other identified features that it deserves special attention.

The 6307 Å feature is visible in ground-based spectra, despite being blended with atmospheric O_2 absorption and emission from the surrounding ejecta. We encourage our colleagues in the Southern Hemisphere to look for it, since it varies between spectroscopic events, and tracking these variations with better temporal sampling may help provide further insight into the 5.5 yr cycle or the recent dramatic brightening of the central star.

This work made use of the NIST Atomic Spectra Database[11] and the Kentucky Atomic Line List, version 2.04.[12] We also wish to thank M. Salvo (ANU) for generously using some of her time on the MSO 2.3 m telescope to obtain current ground-based spectra for us. T. R. Gull (NASA GSFC) prepared most of the detailed STIS observing plans and gave other valuable help in the Treasury Program. Meanwhile, K. Ishibashi (MIT) produced the improved reduction software and contributed to the observing plans. We also thank S. Johansson, H. Hartman (University of Lund), and M. Bautista (Instituto Venezolano de Investigaciones Científicas) for comments on an early version of this paper, and Beth Periello (STScI) for assistance with the *HST* observing plan.

[11] See http://physics.nist.gov/PhysRefData/ASD/index.html.
[12] See http://www.pa.uky.edu/~peter/atomic/index.html.

REFERENCES

Damineli, A., Stahl, O., Kaufer, A., Wolf, B., Quast, G., & Lopes, D. F. 1998, A&AS, 133, 299
Davidson, K. 2004, STScI Newsl., 21(2), 1, http://sco.stsci.edu/newsletter/PDF/2004/spring_04.pdf
Davidson, K., et al. 1999, AJ, 118, 1777
———. 2005, AJ, 129, 900
Hofmann, K.-H., & Weigelt, G. 1988, A&A, 203, L21
Johansson, S., & Hamann, F. W. 1993, Phys. Scr., T47, 157
Martin, J. C., & Koppelman, M. D. 2004, AJ, 127, 2352
Martin, J. C., et al. 2006, ApJ, 640, 474
Sirianni, M., et al. 2005, PASP, 117, 1049
Smith, N., Davidson, K., Gull, T. R., Ishibashi, K., & Hillier, D. J. 2003, ApJ, 586, 432
Stahl, O., Weis, K., Bomans, D. J., Davidson, K., Gull, T. R., & Humphreys, R. M. 2005, A&A, 435, 303
Steiner, J. E., & Damineli, A. 2004, ApJ, 612, L133
Thackeray, A. D. 1953, MNRAS, 113, 211
Wallerstein, G., Gilroy, K. K., Zethson, T., Johansson, S., & Hamann, F. 2001, PASP, 113, 1210
Weis, K., Bomans, D. J., Stahl, O., Davidson, K., Humphreys, R. M., & Gull, T. R. 2005b, in ASP Conf. Ser. 332, The Fate of the Most Massive Stars, ed. R. Humphreys & K. Stanek (San Francisco: ASP), 162
Weis, K., Stahl, O., Bomans, D. J., Davidson, K., Gull, T. R., & Humphreys, R. M. 2005a, AJ, 129, 1694
Whitelock, P. A., Feast, M. W., Marang, F., & Breedt, E. 2004, MNRAS, 352, 447
Zethson, T. 2001a, Ph.D. thesis, Lund Univ.
Zethson, T., Hartman, H., Johansson, S., Gull, T., Ishibashi, K., & Davidson, K. 2001b, in ASP Conf. Ser. 242, Eta Carinae and Other Mysterious Stars: The Hidden Opportunities of Emission Spectroscopy, ed. T. R. Gull, S. Johannson, & K. Davidson (San Francisco: ASP), 97